

1 **TITLE**

2 Fully automated histological classification of cell types and tissue regions of celiac disease is
3 feasible and correlates with the Marsh score

4

5 **AUTHORS**

6 Michael GRIFFIN¹, M.S., michael.griffin@pathai.com

7 Aaron M. GRUVER², M.D., Ph.D., gruver_aaron_m@lilly.com

8 Chintan SHAH¹, M.S., chintan.shah@pathai.com

9 Qasim WANI¹, B.S., qasim.wani@pathai.com

10 Darren FAHY¹, B.S., darren.fahy@pathai.com

11 Archit KHOSLA¹, M.S., archit.khosla@pathai.com

12 Christian KIRKUP¹, M.S., christian.kirkup@pathai.com

13 Daniel BORDERS¹, M.S., daniel.borders@pathai.com

14 Jacqueline A. BROSNAN-CASHMAN¹, Ph.D., jackie.brosnancashman@pathai.com

15 Angie D. FULFORD², M.S., fulford_angie_d@lilly.com

16 Kelly M. CREDILLE², D.V.M, Ph.D., credille_kelly_m@lilly.com

17 Christina JAYSON¹, Ph.D., christina.jayson@pathai.com

18 Fedaa NAJDAWI^{1,*}, M.D., fedaa.najdawi@pathai.com

19 Klaus GOTTLIEB^{2,*}, M.D., Ph.D., klaus.gottlieb@lilly.com

20 * Fedaa Najdawi and Klaus Gottlieb contributed equally as co-senior authors

21

22 **AUTHORS' AFFILIATIONS**

23 ¹ PathAI, Boston, MA, USA

24 ² Eli Lilly and Company, Indianapolis, IN, USA

25

26

27 **AUTHOR FOR CORRESPONDENCE**

28 Fedaa Najdawi

29 PathAI, Inc.

30 1325 Boylston Street, Suite 10000

31 Boston, MA 02215

32 USA

33 Tel: +1-617-500-8457

34 Email: fedaa.najdawi@pathai.com

35

36

37

38

39

40

41

42

43

44

45

46

47

48 **ABSTRACT**

49 **Aims** Histological assessment is essential for the diagnosis and management of celiac
50 disease. Current scoring systems, including modified Marsh (Marsh–Oberhuber) score, lack
51 inter-pathologist agreement. To address this unmet need, we aimed to develop a fully
52 automated, quantitative approach for histology characterisation of celiac disease.

53 **Methods** Convolutional neural network models were trained using pathologist
54 annotations of haematoxylin and eosin-stained biopsies of celiac disease mucosa and
55 normal duodenum to identify cells, tissue and artifact regions. Human interpretable features
56 were extracted and the strength of their correlation with Marsh scores were calculated using
57 Spearman rank correlations.

58 **Results** Our model accurately identified cells, tissue regions and artifacts, including
59 distinguishing intraepithelial lymphocytes and differentiating villous epithelium from crypt
60 epithelium. Proportional area measurements representing villous atrophy negatively
61 correlated with Marsh scores ($r=-0.79$), while measurements indicative of crypt hyperplasia
62 and intraepithelial lymphocytosis positively correlated ($r=0.71$ and $r=0.44$, respectively).
63 Furthermore, features distinguishing celiac disease from normal colon were identified.

64 **Conclusions** Our novel model provides an explainable and fully automated approach for
65 histology characterisation of celiac disease that correlates with modified Marsh scores,
66 facilitating diagnosis, prognosis, clinical trials and treatment response monitoring.

67 **KEYWORDS**

68 MeSH terms:

- 69
- 70 • Artificial intelligence
 - 71 • Celiac disease
 - 72 • Histology
 - 73 • Machine learning

74 **KEY MESSAGES**

75 What is already known on this topic

76 ➤ Prior research has utilised machine learning (ML) techniques to detect celiac disease
77 and evaluate disease severity based on Marsh scores.

78 ➤ However, existing approaches lack the capability to provide fully explainable tissue
79 segmentation and cell classifications across whole slide images in celiac disease
80 histology.

81 ➤ The need for a more comprehensive and interpretable ML-based method for celiac
82 disease diagnosis and characterisation is evident from the limitations of currently
83 available scoring systems as well as inter-pathologist variability.

84 What this study adds

85 ➤ This study is the first to introduce an explainable ML-based approach that provides
86 comprehensive, objective celiac disease histology characterisation, overcoming inter-
87 observer variability and offering a scalable tool for assessing disease severity and
88 monitoring treatment response.

89 How this study might affect research, practice or policy

90 ➤ This study's fully automated and ML-based histological analysis, including the
91 correlation of Marsh scores, has the potential to enable more precise disease severity
92 measurement, risk assessment and clinical trial endpoint evaluation, ultimately
93 improving patient care.

94 INTRODUCTION

95 Celiac disease, an autoimmune disease triggered by dietary gluten, affects around 1% of the
96 population.¹ Its diagnosis can be challenging due to symptom diversity, spanning from no
97 symptoms to severe malabsorption.^{1 2} Patients with celiac disease face a slightly increased
98 overall risk of developing bowel lymphoma in comparison to the general population.²

99 Histological assessment is crucial for the diagnosis and management of celiac
100 disease,³ as well as for endpoint assessment in clinical trials,⁴ with findings of intraepithelial
101 lymphocytosis, crypt hyperplasia and villous atrophy indicative of the presence of the
102 disease.⁵ Clinical study endpoints often rely on a quantification of disease activity,
103 demonstrated by changes in histology and characterised according to disease severity by
104 classification systems such as the modified Marsh (Marsh–Oberhuber) score.^{3 6} However,
105 inter-observer agreement is low for these metrics.⁶ The United States Food and Drug
106 Administration recommends using a clinically accepted histological scale such as the Marsh
107 score for screening samples in clinical studies of treatments for celiac disease, to ensure
108 patient eligibility at enrolment. Furthermore, histology is also recommended as a co-primary
109 endpoint in these studies.⁷

110 Celiac disease is often underdiagnosed due to variation between pathologists in their
111 assessment of biopsy tissue samples,⁸ even if multiple biopsies are obtained.^{3 5} Poor quality
112 of biopsy tissue and overlapping histopathology features between related conditions may
113 contribute to this variability.^{5 8 9} Recently, there has been increased interest in applying
114 machine learning (ML) to pathology,^{10 11} including to improve the accuracy and efficiency of
115 celiac disease diagnosis.¹²

116 Such automation is expected to significantly reduce variability,^{12 13} enabling smaller
117 clinical studies to attain sufficient statistical power to demonstrate treatment effects. Indeed,
118 convolutional neural network (CNN) tissue and cell model predictions from gastrointestinal
119 samples have been used to create human interpretable features (HIFs) that enable the

120 quantitative assessment of inflammatory pathological changes in non-celiac gastrointestinal
121 diseases.¹⁶

122 While previous research has successfully employed ML to detect celiac disease and
123 assess disease severity based on Marsh scores,¹³ this study aims to bridge critical gaps in
124 the current research landscape. The work presented here represents the first report of an ML
125 application for celiac disease that provides fully explainable tissue segmentation and cell
126 classifications across whole slide images (WSIs) of duodenal mucosal biopsies. Through this
127 approach, we have enabled the extraction of HIFs, such as cell densities, cell count
128 proportions, and tissue area proportions, all of which exhibit correlations with Marsh scores.
129 By utilising ML-based quantification, this study aims to objectively and exhaustively
130 characterise celiac disease histology, address the limitations of manual histological
131 assessments, and provide granular data for translational research and clinical trials. We
132 believe such an approach has tremendous potential as a scalable tool for measuring disease
133 severity and monitoring treatment response.

134

135 **MATERIALS AND METHODS**

136 **Data set characteristics**

137 WSIs of haematoxylin and eosin (H&E)-stained biopsies of duodenal mucosa of varying
138 celiac disease severity (N=318) and mucosa of normal duodenum (N=58) were collected
139 from PathAI Diagnostics (Memphis, USA) (**supplemental figure 1**).

140 The cohort size was determined based on the project's scope and the availability of
141 small intestine biopsies encompassing the full spectrum of celiac disease histology at the
142 central laboratory. Slides were scanned at 40x objective magnification using the Aperio
143 GT450 slide scanner (Leica Biosystems, Wetzlar, Germany). Celiac disease slides were split
144 into training (n=230; 72.3%), validation (n=60; 18.9%) and test (n=28; 8.8%) datasets to
145 ensure the even distribution of available patient metadata. For normal duodenum, slides
146 were divided into a similar ratio of training (n=40; 69.0%), validation (n=12; 20.7%) and test
147 (n=6; 10.3%) datasets.

148 **Machine learning-based tissue model development**

149 We developed a model to identify and quantify relevant tissue regions, and we also utilised a
150 previously trained model to identify and quantify cell types and artifact regions¹⁶ on H&E-
151 stained WSIs of celiac disease and normal duodenum (**figure 1**). Using these identified cells
152 and tissue regions, histological features relevant to celiac disease and representing
153 surrogate measures of modified Marsh score components were quantified, including the
154 proportion of intraepithelial lymphocytes to enterocytes in villous epithelium and the surface
155 areas of villous epithelium and crypt epithelium. The latter two features assess villous height
156 and crypt hyperplasia respectively.

157 WSIs were annotated by board-certified gastrointestinal pathologists. In total, 8356
158 tissue region annotations were collected. Annotations of crypt epithelium, villous epithelium,
159 crypt lumen, lamina propria, blood vessels, muscularis mucosa and other tissue (including
160 Brunner's glands and submucosa) were used to train a HIF-based tissue segmentation

161 region model. From these annotations, a CNN model was trained to produce pixel-level
162 predictions of small intestinal mucosa tissue regions. Previously developed models to detect
163 and exclude tissue artifacts and identify and classify the cells in colon tissue were also
164 deployed.¹⁶ Tissue and cell model predictions were visualised as heatmaps on WSIs.
165 Heatmap transformations were used to remove artifact regions (e.g. debris, tissue folds, out-
166 of-focus regions), extracting features only from high-quality tissue.

167 **Validation and review of cell and tissue models**

168 A PathAI pathologist (F.N.) performed quality control of the tissue labels used for model
169 training and qualitatively reviewed the tissue and cell overlays representing model
170 predictions on H&E-stained WSIs. This qualitative review helped guide the iterative model
171 development (**supplemental figure 2**).

172 To establish ground truth for cell model prediction accuracy, representative image
173 frames were sampled (75 μm \times 75 μm ; N=160). Frames were exhaustively annotated for all
174 model-predicted cell types by five gastrointestinal pathologists. Hierarchical clustering was
175 performed on these annotations and model predictions as previously described to identify
176 cell locations.¹⁶ To account for potential pathologist bias and variability, Bayesian-estimated
177 ground truths were used to quantify and compare the performance of the annotators and the
178 model (**supplemental figure 3**).

179 **Evaluation of model-derived HIFs**

180 HIFs (e.g. the proportional area of villous epithelium relative to lamina propria) were
181 extracted from WSIs of normal duodenum (N=52) and scored celiac disease (N=118). HIFs
182 were correlated with modified Marsh scores (type 0, normal lesions; type 1, infiltrative
183 lesions; type 2, hyperplastic lesions; and types 3a, 3b and 3c, destructive lesions)⁶ using
184 Spearman rank correlations. Scores only assessed the presence of >30 intraepithelial
185 lymphocyte cells when differentiating scores 0 from 1 rather than quantifying any further
186 increase in intraepithelial lymphocyte cells with increasing disease severity.

187 After establishing correlations between HIFs and modified Marsh scores, potential
188 differences in the model-derived features between celiac disease and normal duodenum
189 were evaluated.

190 **Statistical analysis**

191 To assess cell model performance, the harmonised average of precision and sensitivity (F1
192 score) was calculated for both the cell model predictions and each pathologist annotation
193 compared to the consensus on representative image frames. To evaluate the model-
194 generated HIFs, each HIF was assessed for correlation with consensus modified Marsh
195 scores using Spearman rank correlations. Data analyses in this study used the programming
196 language Python (OpenEDG Python Institute, West Pomerania, Poland) for tissue and cell
197 model development. Additionally, OpenSlide Python (Carnegie Mellon University, Pittsburgh,
198 PA, USA) was used to load WSIs, Matplotlib (John D Hunter, Matplotlib Development Team
199 and NumFOCUS, Austin, TX, USA) was used for plotting graphs, and PyTorch (PyTorch
200 Foundation, the Linux Foundation, San Francisco, CA, USA) was used for tissue and cell
201 model development.

202 To associate model-derived features of celiac disease following correlations with
203 modified Marsh scores, mean (standard deviation) feature levels were used to show
204 differences between celiac disease and normal duodenum. P values were calculated by
205 independent *t*-test.

206 RESULTS

207 Model development for quantitation of celiac disease histological features

208 The tissue model developed, as well as the previously trained cell and artifact models,¹⁶ were
209 deployed on H&E-stained WSIs of celiac disease and normal duodenum. Relevant cell types
210 identified included neutrophils, plasma cells, enterocytes, intraepithelial lymphocytes, non-
211 intraepithelial lymphocytes, eosinophils and goblet cells (**figure 2**); all other cell types are
212 predicted as “other cells”. In addition, tissue regions identified included villous epithelium,
213 crypt epithelium, lamina propria, muscularis mucosa and blood vessels (**figure 3**). Tissue
214 regions such as total epithelium and mucosa could also be extracted from the tissue
215 segmentation overlays. The tissue model distinguished villous epithelium from crypt
216 epithelium.

217 The cell model’s performance was validated by comparing it with pathologists’
218 annotations using Bayesian-estimated ground truths. Here, we sought to concentrate this
219 validation on overlapping cells, focusing on cell confusion. The cell model demonstrated
220 acceptable sensitivity for most cell types (**figure 4**).

221 Cell model predictions were compared with labels from five gastrointestinal
222 pathologists on representative image frames to determine model accuracy. We reported
223 elements of the F1 score for both cell model predictions and pathologists’ labels for each of
224 the cell types (**figure 5A,B**). Overall, cell model specificity remained relatively consistent and
225 was similar to that of the pathologists for most cell types, with a slight difference being seen
226 for plasma cells, while sensitivity was more variable outside the intraepithelial lymphocyte
227 class.

228 Correlation of surrogate features with modified Marsh score

229 HIFs from our models were analysed to assess correlation with modified Marsh scores. The
230 area of villous epithelium relative to mucosa was negatively correlated with modified Marsh
231 score (Spearman $r=-0.79$, $p<0.0001$) (**figure 6A**). The area of crypt epithelium in tissue

232 (figure 6B) positively correlated with modified Marsh score (Spearman $r=0.71$, $p<0.0001$), as
233 did the number of intraepithelial lymphocyte cells relative to enterocyte cells in villous
234 epithelium (figure 6C) (Spearman $r=0.44$, $p<0.0001$). These results are summarised in
235 **supplemental table 1**.

236 The HIFs extracted from the cell and tissue models distinguished normal biopsies from
237 those with celiac disease. For example, the proportional area of villous epithelium relative to
238 mucosa and the proportional area of villous epithelium relative to crypt epithelium were both
239 lower in celiac disease tissue compared with normal tissue, while the proportional area of
240 crypt epithelium relative to total epithelium, the proportional area of lamina propria over
241 mucosa and the density of intraepithelial lymphocytes in villous epithelium were higher in
242 celiac disease ($p<0.0001$ for all comparisons) (table 1).

243 **Table 1** Association of model-derived features with celiac disease

	Feature	Normal duodenum	Celiac disease	P value
		Mean (SD)	Mean (SD)	
Features quantifying villous atrophy	Area proportion of villous epithelium over mucosa in tissue	0.33 (0.08)	0.15 (0.07)	<0.0001
	Area proportion of villous epithelium over all epithelium in tissue	0.58 (0.10)	0.36 (0.14)	<0.0001
	Area proportion of villous epithelium over lamina propria in tissue	1.11 (0.35)	0.36 (0.23)	<0.0001
Features quantifying crypt hyperplasia	Area proportion of crypt epithelium over usable tissue	0.21 (0.05)	0.23 (0.07)	0.12
	Area proportion of lamina propria over crypt epithelium in tissue	1.38 (0.49)	1.90 (0.82)	<0.0001
	Area proportion of crypt epithelium over all epithelium in tissue	0.42 (0.10)	0.64 (0.14)	<0.0001
	Area proportion of crypt epithelium over mucosa in tissue	0.24 (0.05)	0.27 (0.07)	<0.01
Surrogate features for villous height/ crypt depth ratio	Area proportion of villous epithelium over crypt epithelium in tissue	1.54 (0.87)	0.64 (0.47)	<0.0001
Features quantifying intraepithelial lymphocyte infiltration	Count proportion of intraepithelial lymphocytes over enterocytes in villous epithelium	0.20 (0.07)	0.31 (0.11)	<0.0001
	Density of intraepithelial lymphocytes in villous epithelium	910.27 (303.15)	1446.27 (463.91)	<0.0001
Features quantifying expansion of inflammatory cells in lamina propria	Count proportion of plasma cells over all cells in lamina propria	0.23 (0.05)	0.29 (0.10)	<0.001
	Density of plasma cells in lamina propria	2131.66 (593.54)	2725.74 (1171.97)	<0.001
	Density of lymphocytes in lamina propria	2483.02 (793.40)	1808.05 (641.31)	<0.0001
	Count proportion of lymphocytes over all cells in lamina propria	0.27 (0.06)	0.19 (0.06)	<0.0001

	Area proportion of lamina propria over mucosa in tissue	0.31 (0.04)	0.47 (0.08)	<0.0001
	Total number of cells in lamina propria	54,013.02 (28142.69)	89,593.13 (50,629.86)	<0.0001
Other features quantifying inflammatory cells	Count proportion of neutrophils over all cells in mucosa	0.03 (0.01)	0.05 (0.02)	<0.0001
	Count proportion of eosinophils over all cells in mucosa	0.02 (0.01)	0.03 (0.01)	<0.0001

244 SD, standard deviation.

245 **DISCUSSION**

246 Histological assessment of celiac disease plays a crucial role in diagnosing disease and
247 evaluating the effectiveness of clinical interventions.³ However, inter-observer variability can
248 affect the consistency and accuracy of results.⁶ To overcome this limitation and augment
249 pathologists' assessments of disease severity, we aimed to develop a fully automated and
250 explainable approach to quantify the cellular and tissue-based features of celiac disease in
251 H&E-stained clinical samples. The HIFs extracted from this model reflected histological
252 changes that were measured by modified Marsh scores, potentially providing a quantitative
253 and reproducible means to assess celiac disease severity.

254 Our model produced continuous feature measurements that can be interpreted as
255 surrogate markers of celiac disease pathology (**supplemental table 1**). The relationship of
256 these features with the ordinal Marsh score categories can be used as a benchmark to
257 measure the model's performance. For example, we examined the area of villous epithelium
258 relative to the area of mucosa as an indicator of villous blunting, a hallmark of celiac disease,
259 and found a negative correlation with higher modified Marsh scores. To gauge crypt
260 hyperplasia, a more subtle feature, we examined the area of crypt epithelium relative to total
261 epithelial area, revealing a positive correlation between this feature and Marsh scores at a
262 Marsh score of 2 and above. The trained cell model directly quantitated the proportion of
263 intraepithelial lymphocytes relative to the number of enterocytes within the villous structures.
264 As expected, these values increased with disease severity.

265 Existing celiac disease scoring systems, such as the modified Marsh score, primarily
266 rely on qualitative and descriptive categorisations, leading to subjectivity and limited
267 sensitivity to subtle changes.¹⁷ In this study, we propose an alternative approach, utilising ML
268 techniques to enable continuous, quantitative evaluation of the histological changes in celiac
269 disease. By capturing histological alterations on a granular and objective scale, this novel
270 approach offers enhanced sensitivity to changes in intraepithelial lymphocyte density, as well

271 as villous and crypt epithelial surface area, overcoming limitations of the qualitative
272 assessments of conventional manual scoring systems.

273 Some of our model-extracted HIFs directly quantified features of intraepithelial
274 lymphocytes. This cell type is an essential consideration during disease assessment, as the
275 presence of >30 intraepithelial lymphocytes per 100 enterocytes in the duodenum is a
276 defining feature of celiac disease.¹⁸ The HIFs extracted from our model include count
277 proportions and/or density of intraepithelial lymphocytes, specifically in the villous epithelium.
278 This model also allowed for the extraction of features relating to intraepithelial lymphocytes in
279 crypt epithelium and a comparison of their density in villous and crypt epithelium, providing a
280 comprehensive overview of the spatial distribution of this cell type within distinct epithelial
281 regions. Additional relevant features included the proportional area of villous epithelium
282 (quantifying the change related to villous atrophy), the proportional area of crypt epithelium
283 (quantifying crypt hyperplasia) and the ratio of villous epithelium area to crypt epithelium area
284 (quantitatively capturing the relationship of villous height to crypt depth).¹⁹

285 The key strengths of this study become apparent when considering that these model-
286 generated features not only bear relevance to the modified Marsh scoring system but are
287 also essential components of the histological hallmarks of celiac disease (**table 1**).¹⁹ These
288 HIFs encompass features not previously incorporated into any formalised scoring system,
289 such as relative numbers and density of inflammatory cells (including lymphocytes, plasma
290 cells, eosinophils and neutrophils) in lamina propria or in mucosa. These metrics
291 characterise the immune micro-environment within celiac biopsies, as well as the total area
292 and area proportion of lamina propria, capturing the expansion of lamina propria, a
293 phenomenon known to be associated with disease activity.¹⁹

294 Furthermore, one of the key strengths of this study lies in our model's capacity to
295 discern between normal duodenum and celiac disease through the quantification of features
296 associated with the disease microenvironment in mucosal biopsies. As expected, quantifying
297 features of villous atrophy, as evidenced by reduced area proportion of this feature, and the

298 augmented area proportion signifying mucosa crypt hyperplasia, distinguished between the
299 histology of unaffected biopsies and those indicative of celiac disease. Supplementary
300 quantitative attributes of the inflammatory microenvironment known to be associated with
301 celiac disease, encompassing the infiltration of chronic inflammatory cells like lymphocytes
302 and plasma cells within the lamina propria, coupled with the associated expansion of this
303 layer,¹⁹ further distinguished normal biopsy samples from those with celiac disease.
304 Discernible differences between the two groups were also observed in the quantitative
305 evaluation of granulocytes, which has been previously described.^{20 21}

306 While our model was limited by the small sample size, additional assessment involving
307 larger cohorts will allow future refinement of the model's performance. The cell model can
308 also be trained specifically on duodenum biopsies and expanded to predict features
309 associated with additional cell types (e.g. Paneth cells). An additional limitation of the current
310 approach is related to the extraction of HIFs across a specific tissue area in the entire slide,
311 which overlooks the potential variation between different tissue fragments. In a manual
312 assessment of celiac disease in biopsies, pathologists often determine disease severity
313 based on the most severely affected tissue region. To address this limitation, future work will
314 focus on reporting HIFs separately for specific regions of interest within the tissue sample.
315 This strategy is expected to allow for a more comprehensive and accurate assessment of
316 disease severity within distinct tissue regions.

317 We foresee that ML-supported histological analysis will play a pivotal role in the
318 advancement of precision medicine for patients with celiac disease. To our knowledge, this is
319 the first report of fully explainable ML-based tissue and cell classifications across the WSIs of
320 mucosal biopsies in celiac disease, enabling the extraction and statistical analysis of HIFs to
321 empower translational research and clinical trials. The resulting quantitative model-generated
322 HIFs can be used to build predictive models of existing Marsh scores or function as a
323 continuous measurement, tracking histological change in celiac biopsies. Expanding upon
324 this foundation, as we proceed to develop classification models aimed at predicting clinical

325 outcomes alongside slide-level scores, we anticipate that the interpretability enabled by the
326 utilisation of HIFs is poised to serve a dual purpose: validating the integrity of these models
327 and revealing novel insights into disease biology. We believe that this ML-based assessment
328 has tremendous potential as a scalable tool for measuring disease severity, risk stratification,
329 prognostic evaluation, evaluating endpoints in clinical trials and monitoring of treatment
330 responses; ultimately, advancing the care of patients with celiac disease.

331 **Acknowledgements**

332 The authors would like to thank all study participants. The authors are grateful to the
333 software engineering and machine learning teams at PathAI for developing the systems and
334 pipelines used for model development and feature extraction.

335 **Contributors**

336 MG: conceptualisation, data curation, formal analysis, investigation, methodology, project
337 administration, supervision, validation and visualisation, AMG: funding acquisition and writing
338 (review and editing), CS: conceptualisation, data curation, formal analysis, investigation,
339 methodology, validation and visualisation, QW: conceptualisation, data curation, formal
340 analysis, investigation, methodology, validation and visualisation, DF: data curation, AK:
341 conceptualisation, investigation, methodology, software and writing (review and editing), CK:
342 conceptualisation, data curation and writing (review and editing), DB: conceptualisation,
343 investigation, formal analysis and writing (review and editing), JABC: writing (original draft)
344 and writing (review and editing), CJ: conceptualisation, data curation, formal analysis,
345 investigation, methodology, project administration, validation and visualisation, FN:
346 conceptualisation, data curation, formal analysis, investigation, methodology, project
347 administration, validation, visualisation, writing (original draft) and writing (review and
348 editing), KG: conceptualisation, funding acquisition, supervision and writing (review and
349 editing). All authors: final approval of the manuscript. FN and KG are joint last authors.

350 **Funding support**

351 This study was sponsored by Eli Lilly and Company. Medical writing assistance was provided
352 by Jason Vuong, BPharm, and Clare Weston, MSc, of ProScribe – Envision Pharma Group,
353 and was funded by Eli Lilly and Company. ProScribe's services complied with international
354 guidelines for Good Publication Practice.

355 **Role of the sponsor**

356 Eli Lilly and Company was involved in the study design, oversight and preparation of the
357 manuscript.

358 **Competing interests**

359 AMG, ADF, KMC and KG are employees and shareholders of Eli Lilly and Company.

360 MG, CS, QS, DF, AK, CK, DB, JABC, CJ and FN are employees of PathAI.

361 **Patient consent for publication**

362 Not required.

363 **Ethics approval**

364 WCG IRB protocol number: 1316112

365 **Data availability statement**

366 Model parameters for cell and tissue models, and codes for model training, inference and
367 feature extractions are not disclosed. Access requests for such code will not be considered
368 to safeguard PathAI's intellectual property. All feature tables, as well as source code, for
369 reproducing correlational analyses will be deposited to GitHub prior to publication, and the
370 link will be provided at that time. Access to cell- and tissue-type heatmaps, as well as usage
371 of cell- and tissue-type classification models, are available on reasonable request to
372 academic investigators, without relevant conflicts of interest, for non-commercial use who
373 agree not to distribute the data. Access requests can be made to: publications@pathai.com.

REFERENCES

- 1 Lebwohl B, Sanders DS, Green PHR. Coeliac disease. *Lancet* 2018;391:70–81.
- 2 Marafini I, Monteleone G, Stolfi C. Association between celiac disease and cancer. *Int J Mol Sci* 2020;21:4155.
- 3 Rubio-Tapia A, Hill ID, Kelly CP, *et al.* ACG clinical guidelines: diagnosis and management of celiac disease. *Am J Gastroenterol* 2013;108:656–76.
- 4 Gottlieb K, Dawson J, Hussain F, *et al.* Development of drugs for celiac disease: review of endpoints for phase 2 and 3 trials. *Gastroenterol Rep (Oxf)* 2015;3:91–102.
- 5 Green PH, Cellier C. Celiac disease. *N Engl J Med* 2007;357:1731–43.
- 6 Corazza GR, Villanacci V, Zambelli C, *et al.* Comparison of the interobserver reproducibility with different histologic criteria used in celiac disease. *Clin Gastroenterol Hepatol* 2007;5:838–43.
- 7 US Food & Drug Administration (FDA). Celiac disease: developing drugs for adjunctive treatment to a gluten-free diet. 2022. <https://www.fda.gov/regulatory-information/search-fda-guidance-documents/celiac-disease-developing-drugs-adjunctive-treatment-gluten-free-diet> (accessed May 2023).
- 8 Mubarak A, Nikkels P, Houwen R, *et al.* Reproducibility of the histological diagnosis of celiac disease. *Scand J Gastroenterol* 2011;46:1065–73.
- 9 Syed S, Ehsan L, Shrivastava A, *et al.* Artificial intelligence-based analytics for diagnosis of small bowel enteropathies and black box feature detection. *J Pediatr Gastroenterol Nutr* 2021;72:833–41.
- 10 Rakha EA, Toss M, Shiino S, *et al.* Current and future applications of artificial intelligence in pathology: a clinical perspective. *J Clin Pathol* 2021;74:409–14.
- 11 Harrison JH, Gilbertson JR, Hanna MG, *et al.* Introduction to artificial intelligence and machine learning for pathology. *Arch Pathol Lab Med* 2021;145:1228–54.
- 12 Wei JW, Wei JW, Jackson CR, *et al.* Automated detection of celiac disease on duodenal biopsy slides: a deep learning approach. *J Pathol Inform* 2019;10:409–14.

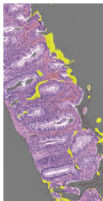
- 13 Koh JEW, De Michele S, Sudarshan VK, *et al.* Automated interpretation of biopsy images for the detection of celiac disease using a machine learning approach. *Comput Methods Programs Biomed* 2021;203:106010.
- 14 Syed S, Al-Boni M, Khan MN, *et al.* Assessment of machine learning detection of environmental enteropathy and celiac disease in children. *JAMA Netw Open* 2019;2:e195822.
- 15 Sali R, Ehsan L, Kowsari K, *et al.* CeliacNet: celiac disease severity diagnosis on duodenal histopathological images using deep residual networks. *Proceedings (IEEE Int Conf Bioinformatics Biomed)* 2019;2019:962–67.
- 16 Najdawi F, Sucipto K, Mistry P, *et al.* Artificial intelligence enables quantitative assessment of ulcerative colitis histology. *Mod Pathol* 2023;36:100124.
- 17 Adelman DC, Murray J, Wu TT, *et al.* Measuring change in small intestinal histology in patients with celiac disease. *Am J Gastroenterol* 2018;113:339–47.
- 18 Bao F, Green PH, Bhagat G. An update on celiac disease histopathology and the road ahead. *Arch Pathol Lab Med* 2012;136:735–45.
- 19 Dickson BC, Streutker CJ, Chetty R. Coeliac disease: an update for pathologists. *J Clin Pathol* 2006;59:1008–16.
- 20 Moran CJ, Kolman OK, Russell GJ, *et al.* Neutrophilic infiltration in gluten-sensitive enteropathy is neither uncommon nor insignificant: assessment of duodenal biopsies from 267 pediatric and adult patients. *Am J Surg Pathol* 2012;36:1339–45.
- 21 Brown IS, Smith J, Rosty C. Gastrointestinal pathology in celiac disease: a case series of 150 consecutive newly diagnosed patients. *Am J Clin Pathol* 2012;138:42–9.

FIGURE LEGENDS

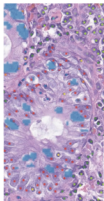
- Figure 1** Proof-of-concept development of models based on HIFs on training data. CNN, convolutional neural network; H&E, haematoxylin and eosin; HIF, human interpretable feature; WSI, whole slide image.
- Figure 2** Overlays generated by cell segmentation model for model deployment.
- Figure 3** Tissue segmentation model showing distinct tissue regions. CD, celiac disease; ND, normal duodenum.
- Figure 4** Cell model confusion matrix showing sensitivity across different cell types.
- Figure 5** Accuracy of cell model predictions compared with pathologists. (A) Specificity comparison. (B) Sensitivity comparison.
- Figure 6** Example cell and tissue segmentation model correlation with modified Marsh score. (A) Surrogate features of villous blunting. (B) Surrogate features of crypt hyperplasia. (C) Surrogate features of intraepithelial lymphocyte infiltration.

Step 1. Deployment

Deploy existing colon artifact, cell and goblet cell cytoplasm models



Artifact detection

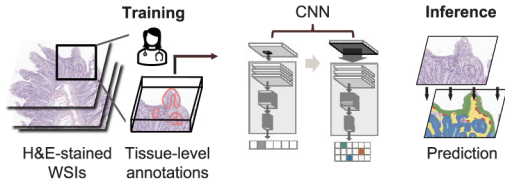


Cell identification



Step 2. Training and inference

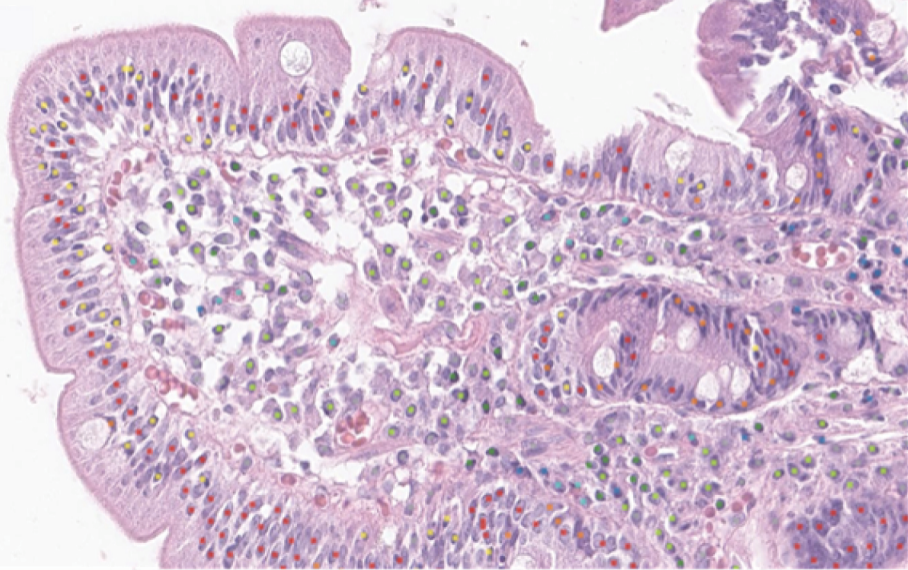
Collect annotations of crypt epithelium, villous epithelium, lumen, lamina propria and muscularis mucosa to train an HIF-based tissue region model



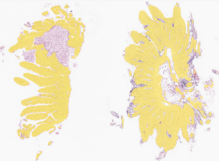
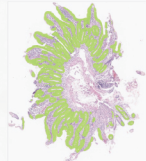
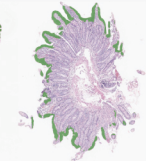
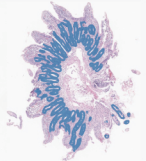
Step 3. Feature extraction

Develop read-outs to quantitate relevant histological features

Substance	Features
Neutrophils	Surface area of villous epithelium
Crypt epithelium	Surface area of crypt epithelium
Plasma cells	Count proportion of intraepithelial lymphocytes to enterocytes
Villous epithelium	
Intraepithelial lymphocytes	



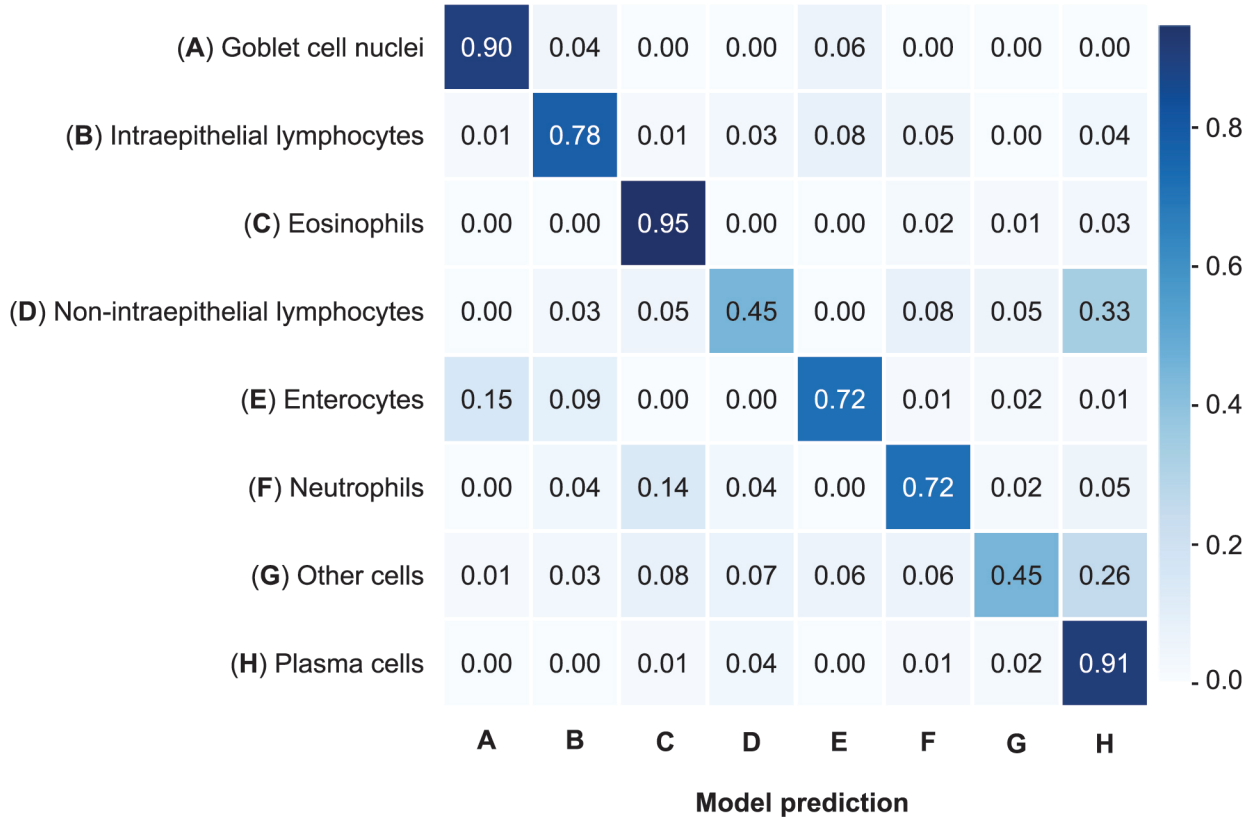
- Goblet cell nuclei
- Enterocytes
- Intraepithelial lymphocytes
- Non-intraepithelial lymphocytes
- Plasma cells
- Eosinophils
- Neutrophils
- Other cells

A**B****C****D**

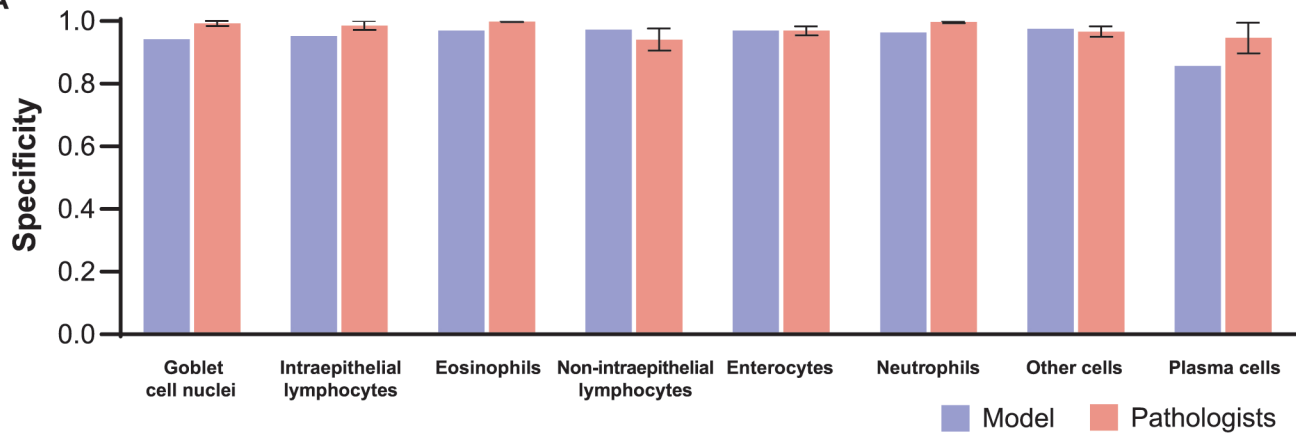
Overlay showing ND (left)
vs. CD (right) in:

- (A)** Mucosa
- (B)** All epithelium
- (C)** Villous epithelium
- (D)** Crypt epithelium

Ground truth



A



B

